BMC Cancer

RESEARCH

Open Access

Combining network pharmacology and experimental verification to explore the inhibitory effects of Deoxyelephantopin (DET) Against Non-Small Cell Lung Cancer (NSCLC)

Shenjia Wu[1,2†], Ying Guo[1,2†] and Rong Wang[1,2*]

Abstract

Background DET has a significant inhibitory activity against a range of cancer cells; however, its specific effects and underlying mechanisms in Non-Small Cell Lung Cancer (NSCLC) remain to be fully elucidated. This study aimed to investigate the potential mechanisms through which DET exerts its anti-neoplastic effects on NSCLC.

Method Targets of DET were predicted using the SwissTargetPrediction database. Disease targets for NSCLC were obtained from the GeneCards database, and the intersection between drug targets and disease targets was determined. The STRING database was then employed to construct a protein–protein interaction (PPI) network and analyze target interactions. Additionally, Gene Ontology (GO) and Kyoto Encyclopedia of Genes and Genomes (KEGG) enrichment analyses were conducted to investigate their biological functions. Molecular docking simulations were conducted using AutoDock software to analyze the binding interactions between DET and key target proteins. Subsequently, both in vitro and in vivo experiments were carried out to evaluate the anticancer effects of DET, with alterations in key gene expression levels assessed through RT-qPCR and Western blot analyses.

Results A total of 52 potential targets were discovered for DET and NSCLC. The PPI analysis revealed 5 hub targets, including CASP3, PTGS2, TNFα, ICAM1 and JUN. GO analysis identified 164 biological processes, 44 molecular functions and 40 cellular components. KEGG analysis revealed that DET anticancer effects were mediated through multiple pathways, primarily the AGE-RAGE and TNF signaling pathways. Experimental results demonstrated that DET inhibited the proliferation and migration of H460 cells and induced apoptosis in vitro. RT-qPCR and WB indicated that DET up regulated Bax and CASP3 while down regulating Bcl2, JUN, TNFα, NF-κB, ICAM1 and PTGS2.

Conclusion This study aims to investigate the inhibitory effect of DET on NSCLC by combining network pharmacology and experimental methods. The results demonstrate that DET effectively inhibited the proliferation of H460 cells and induced apoptosis, with significant involvement of the AGE-RAGE and TNF signaling pathways, suggesting its potential as a therapeutic intervention for NSCLC.

†Shenjia Wu and Ying Guo contributed equally to this work.

*Correspondence:
Rong Wang
wangrbnu@aliyun.com
Full list of author information is available at the end of the article

Keywords Deoxyelephantopin, NSCLC, Network pharmacology, Apoptosis, Inflammatory factors, Experimental

verification

Introduction

Lung cancer (LC) remains a malignancy characterized by high incidence and mortality rates. Globally, approximately 2.2 million new cases of LC are diagnosed annually, with over 80% of affected individuals succumbing within five years of diagnosis [1, 2]. LC-related deaths account for approximately 18% of total cancer mortality [1]. Based on cellular characteristics, LC is primarily classified into two main categories: small cell lung cancer (SCLC), which represents about 15% of cases, and non-small cell lung cancer (NSCLC), which comprises the remaining 85% [3].

In recent years, treatments such as surgery, chemotherapy, and other therapy have notably enhanced the 5-year survival rates for lung cancer (LC) [4, 5], However, challenges such as significant side effects and the potential for drug resistance persist [6, 7]. Thus, there is a pressing need to discover novel drugs that are efficacious, processes well-defined mechanisms, and exhibit favorable safety profiles. Natural anti-cancer compounds hold promise for tumor treatment due to their superior efficacy, reduced side effects, and lower toxicity [7, 8]. Such as sijunzi decoction [9], osthole [10] and aloin [11].

Natural phytochemicals, regarded as promising anti-tumor agents, have garnered significant interest from researchers. Sesquiterpene lactones, which are bioactive compounds found in nature, have demonstrated both anti-tumor and anti-inflammatory properties [12, 13]. Deoxyelephantopin (DET), a sesquiterpene lactone compound extracted from the *Elephantopus scaber*, has been employed for its anti-inflammatory, antibacterial, antioxidant, and immunomodulatory effects [14]. An increasing amount of research has revealed the pharmacological effects of DET in the treatment of cancer [15]. Ji et al. reported that DET induced colon cancer cell arrest in G2/M phasecell cycle arrest and promoted apoptosis in colon cancer cells, thereby inhibiting their growth. It can also synergize with chemotherapeutic agent 5-Fluorouracil (5-FU) to improve the anti-cancer effect [16]. Ji et al. discovered that DET suppresses the proliferation and migration of pancreatic cancer cells by modulating the linc00511/miR- 370 -5p/p21 promoter axis, as well as inhibiting the growth of mice bearing pancreatic cancer tumors [17]. However, there are limited reports about DET in the treatment of LC, and these primarily focus on cellular-level studies [18–20]. Therefore, the precise function and molecular mechanisms of DET in lung cancer treatment still warrant further investigation.

Network pharmacology represents an advanced method that employs systems biology and bioinformatics to elucidate the complex mechanisms of drug action. This methodology offers a theoretical foundation for the continued exploration of natural products [21, 22]. Consequently, we utilized network pharmacology analysis to pinpoint the potential targets of DET and reveal its intricate mechanisms in the treatment of NSCLC. Molecular docking, a computational method, simulates interactions at the atomic level between molecules and proteins, predicts the conformations of ligand-receptor complexes, and calculates binding affinities, which are essential for evaluating molecular compatibility. This approach is precise and cost-effective, primarily applied in drug design and the study of biochemical pathways [23].

In our research, we employed network pharmacology to investigate the anti-tumor mechanisms of DET and validated our results through in vitro and in vivo experiments, providing experimental reference data for the potential use of DET in NSCLC intervention. The protocol of our study on DET anti-NSCLC procedures is illustrated in Fig. 1.

Material and methods

Targets Collection

The 2 dimensional (2D) molecular structure of DET was obtained from ChemSpider (https://www.chemspider.com/). The potential targets of DET were identified using the SwissTargetPrediction (http://swisstargetprediction.ch/). The targets associated with NSCLC were sourced from the GeneCards (https://www.genecards.org/). Subsequently, the Venny tool (https://bioinfogp.cnb.csic.es/tools/venny/) was employed to identify and visualize the overlapping genes between NSCLC and DET.

PPI network construction

The overlapping genes between DET and NSCLC were inputted into the STRING (https://cn.string-db.org/), with *Homo sapiens* specified as the organism. A minimum confidence level of 0.4 was set to create the PPI network. The resulting network was visualized by Cytoscape v3.9.0 and the network analysis module was employed to perform topological analysis. The color depth and shape size of the nodes were adjusted according to the size of the degree (DC). The DC in the PPI network were

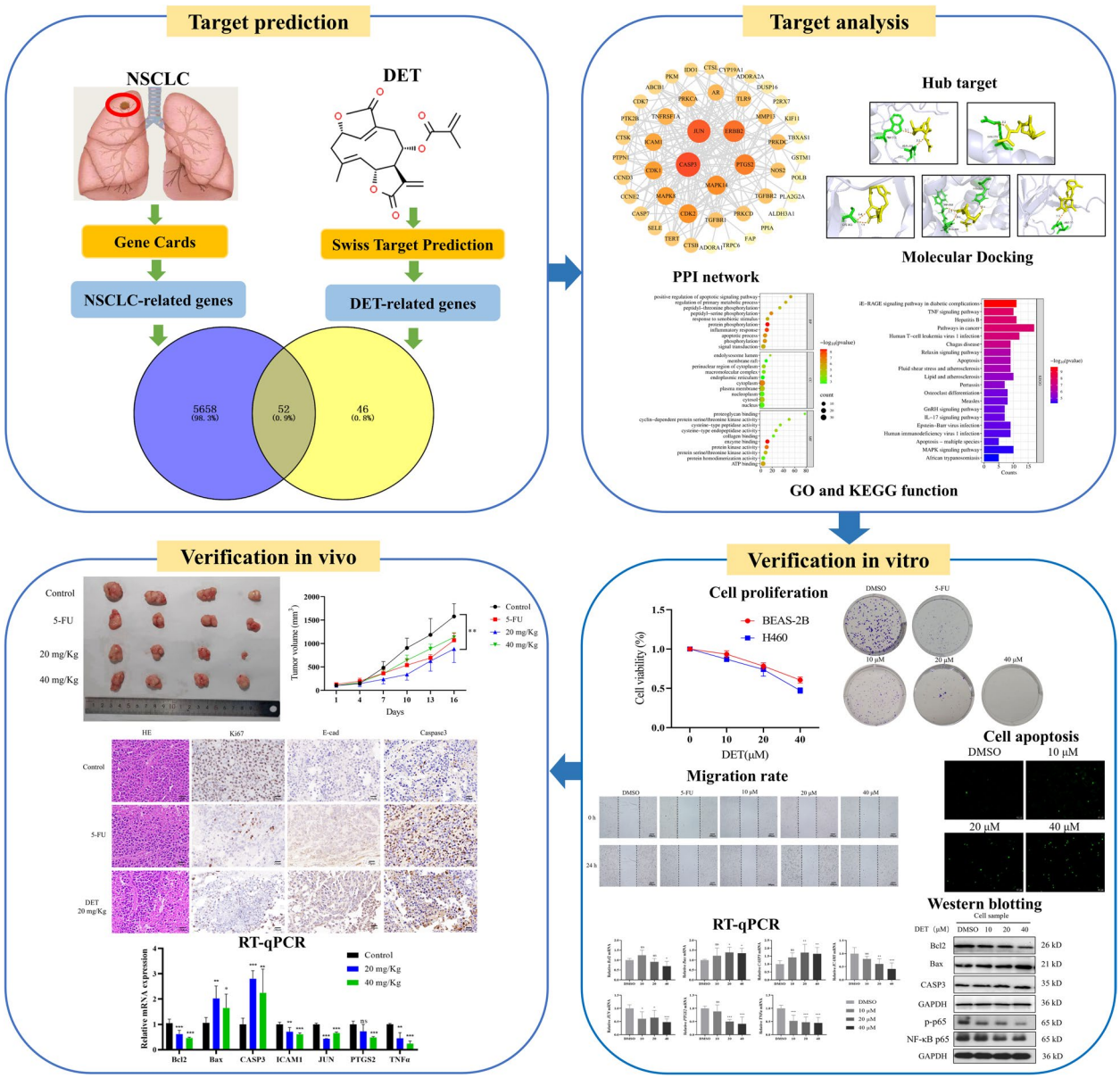

Fig. 1 Flow diagram of the research

arranged from the largest to the smallest, and the top 7 target were selected as the hub targets.

Enrichment analysis

To investigate the GO and KEGG enrichment functions associated with the role of DET in the treatment of NSCLC, we imported the intersection targets of DET and NSCLC into the DAVID database (https://david.ncifcrf.gov/), specifying *Homo sapiens* as the species for the enrichment analysis. The GO analysis was primarily focused on elucidating the functions of gene products across three categories: biological processes (BP), cellular components (CC), and molecular functions (MF). Concurrently, the KEGG pathway enrichment analysis was conducted to identify key pathways and potential biological mechanisms relevant to NSCLC treatment. A *P*-value less than 0.05 was deemed statistically significant for the enrichment results. The resulting GO and KEGG enrichment diagrams were created using an online plotting platform (http://www.bioinformatics.com.cn/).

Molecular docking

Molecular docking was employed to investigate the binding affinities of DET to target proteins. The

three-dimensional (3D) structures of hub target proteins were sourced from Protein Data Bank (PDB) (https://www.rcsb.org/) and processed using PyMOL (https://pymol.org/2/) by removing water molecules and organic ligands. The resulting structures were saved in PDBQT format. Hydrogen atoms were subsequently added to the target protein, which was designated as the receptor, using the AutoDock v1.5.7 software. The 3D structure of DET was acquired from PubChem (https://pubchem.ncbi.nlm.nih.gov/) and prepared using AutoDock v1.5.7, including the addition of hydrogen atoms and the detection of rotatable bonds, with DET selected as the ligand molecule. After adjusting the docking box parameters and completing the settings, the docking process was executed, and the results were visualized using PyMOL. The protein and drug ligand were presented in white and yellow, respectively, while the amino acids interacting with the target protein were highlighted in green.

Cells Lines and reagents

Both the NSCLC cell line H460 and the normal human lung epithelial cell line BEAS- 2B were sourced from the Shanghai Institute of Cell Biology, Chinese Academy of Sciences (Shanghai, China). Deoxyelephantopin (DET) (purity ≥98%, AB2225) was purchased from Chengdu Alfa Biotechnology Co., Ltd (Chengdu, China). Fetal bovine serum (FBS) was bought from (Biological Industries, USA). Dulbecco's modified Eagle's medium (DMEM)/high glucose, 4% paraformaldehyde and Phosphate buffered saline (PBS) were bought from Servicebio Co., Ltd (Wuhan, China). penicillin–streptomycin (PS) was bought from Boster Co., Ltd (Wuhan, China). MTT was obtained from sigma (USA). Dimethyl sulfoxide (DMSO) was bought from Beyotime Co., Ltd (Shanghai, China). Primary antibodies against Bax, Bcl2, CASP3, Ki67, E-cadherin (E-cad), GAPDH and Secondary Antibodies were obtained from Servicebio Co., Ltd (Wuhan, China). Primary antibodies against NF-κB(p65) and p-p65 was bought from Boster Co., Ltd (Wuhan, China). RT-qPCR primers were purchased by the Shanghai Sangon Biotech Co., Ltd (Shanghai, China).

Cells culture and cytotoxic assay

H460 and BEAS- 2B cells were cultured in DMEM supplemented with 10% FBS and 1% penicillin–streptomycin (PS), and maintained in a humidified incubator at 37 °C with 5% CO2 to ensure optimal growth conditions. DET powder was dissolved in DMSO and serially diluted in the culture medium to achieve a final DMSO concentration of 0.1%. The effect of DET on cell viability was assessed using the MTT assay. Cells were seeded in a 96-well plate and treated with various concentrations of DET for 24 h. Subsequently, MTT solution was added and incubated for 4 h. Following this, the culture medium was removed, and DMSO was added. The plate was shaken for 10 min, and the absorbance was detected at 490 nm using a microplate reader (Thermo Fisher, USA). Each group of measurements was conducted in triplicate.

Cell colony formation assay

H460 cells were seeded in 6-well plates at a density of 500 cells per well. Subsequently, cells were treated with various concentrations of DET. 5-FU (40 μM), a first-line chemotherapeutic agent, was selected as the positive control [24]. After 10 days, each well was washed gently with ice-cold PBS, fixed with 4% paraformaldehyde and then stained with crystal violet (Servicebio). Then, the culture plates were washed with PBS to remove the crystal violet stain until the cell colonies became clearly visible. Images were captured, and the colony formation rate was calculated [25]. Each group of data was repeated three times.

Wound healing assay [26]

In the wound healing research, H460 cells were seeded at a density of 5×10^5 cells per well in 6-well plates and allowed to grow until they uniformly covered the bottom of the plates before conducting experiments. Monolayer cells were evenly scratched in a straight line using a 200 μL pipette tip and then treated with DET of different concentrations and cultured at 37℃ with 5% CO_2. Following treatment, the healing of the cell scratches was observed through an microscope (Olympus, Japan) at 0 h and 24 h time points.

Apoptosis assay

Using the TUNEL apoptosis assay kit (Servicebio) to evaluate the apoptosis levels of H460 cells after treatment with DET. H460 cells were seeded in plates and cultured overnight. After 24 h of exposure to various concentrations of DET, under room temperature conditions, immerse in 4% paraformaldehyde for cell fixation, followed by washing with PBS. Then, add the permeable solution and incubate for 5 min. Add the TUNEL detection solution and incubate at 37 °C for 1 h. Remove the detection solution and wash 3 times with PBS. Then, add the DAPI staining solution and incubate for 3 min to stain the nucleus. Finally, the DAPI staining solution was washed away, and the samples were observed and photographed using a fluorescence microscope (Olympus). Fluorescence counting was conducted using image J software.

RNA isolation and RT-qPCR analysis

Total RNA was extracted from tumor cells and tissues samples according to the product instructions for TRIzol

(Servicebio) reagent. The concentration of the purified RNA samples was determined using a NanoDrop 2000 (Thermo Fisher, USA). 800 ng of total RNA was obtained and reverse transcribed into complementary DNA (cDNA) using the First-generation reverse transcription kit (Servicebio). The resulting cDNA was diluted at a ratio of 1:4 to increase the sample volume. SYBR Green qPCR Mix (Servicebio) was used for RT-qPCR analysis, and cDNA amplification was conducted using the 7900HT real-time fluorescence quantitative system (Bio-Rad, USA) to compare gene expression among different experimental groups. All reactions were conducted in triplicate. The data obtained from the experiments were analyzed using the $2^{-\Delta\Delta Ct}$ method, and the expression differences among the groups were compared. The RT-qPCR primers are shown in Table 1.

Western blotting analysis

Total proteins were extracted from tumor cell and tissue samples, and the concentration was detected using a BCA protein assay kit (Servicebio). Proteins with different mass fractions were separated by electrophoresis and transferred to a PVDF membrane. The membrane was blocked with 5% non-fat milk at room temperature for 2 h. Subsequently, Bax, Bcl2, and CASP3 antibodies were diluted at 1:1000 and incubated overnight at 4 °C. The membrane was washed four times with TBST, followed by incubation with a secondary antibody diluted to 1:4000 at room temperature for 1 h, and then washed four times with TBST again. Finally, the PVDF membrane was immersed in ECL luminescent reagent (Servicebio) for 2 min in the dark and detected using a gel imaging system (Alpha Innotech). Protein bands were evaluated and grayscale values determined using Image J software, with the ratio of the target protein to GAPDH indicating the relative expression level.

Table 1 The RT-qPCR primers

Primer	Length	direction	Sequence (5′ → 3′)
GAPDH	136 bp	Forward	AACTTTGGTATCGTGGAAGGACTC
		Reverse	CAGTAGAGGCAGGGATGATGTTC
Bax	88 bp	Forward	ACCAAGAAGCTGAGCGAGTGTC
		Reverse	TGTCCACGGCGGCAATCATC
CASP3	137 bp	Forward	AACAAATGGACCTGTTGACC
		Reverse	CTGTCTCAATGCCACAGTCC
Bcl2	113 bp	Forward	ATGAAATGAGGCGTTGTCACTGTG
		Reverse	CCAGGTCTTGATTCTCGGTCTTCC
PTGS2	94 bp	Forward	AAGTCCCTGAGCATCTACGGTTTG
		Reverse	TGTTCCCGCAGCCAGATTGTG
ICAM1	119 bp	Forward	TCACCTATGGCAACGACTCCTTC
		Reverse	CAGTGTCTCCTGGCTCTGGTTC
JUN	97 bp	Forward	AGAACTCGGACCTCCTCACCTC
		Reverse	ATGTGCCCGTTGCTGGACTG
TNF-α	128 bp	Forward	GGCGTGGAGCTGAGAGATAACC
		Reverse	CGGCTGATGGTGTGGGTGAG

In vivo experiment [27]

The male Balb/c nude mice (5-week-old) utilized in the animal experiments were acquired from GemPharmatech Co., Ltd (Jiangsu, China) and were kept in the Laboratory Animal Center at Fuyang Normal University. After obtaining the BALB/c mice and keeping them for a week, their health was verified to be satisfactory. Then, H460 cells were collected and inoculated into the right axilla of the mice via subcutaneous implantation. Using a caliper to measure the length and width of the tumor, the tumor volume is calculated using the formula (Length $\times$Width^2)/2. when the tumor volume reached 125 mm^3, the mice were randomly divided into four groups. the negative control group received 0.1 ml of PBS containing 0.5% CMC-Na, while those in the DET group were treated with 20 and 40 mg/kg (with DET dissolved in 0.1 ml PBS containing 0.5% CMC-Na at a concentration of 1 μg/μL) and the positive control group received 5-FU at 25 mg/kg. All groups were administered medication via gavage every two days for a total of 16 days. Every three days, the weight and tumor volume of the mice were measured. After the experiment was completed, the mice were euthanized by cervical dislocation to obtain the tumor tissues. Collect tumor samples and divide them into two portions with a blade. One portion is rapidly immersed in liquid nitrogen and stored at − 80 °C for RT-qPCR and WB analysis, while the other portion is fixed in 4% paraformaldehyde for morphological studies.

Hematoxylin–eosin staining and immunohistochemistry

Tumor tissue was immersed in 4% paraformaldehyde for 24 h, dehydrated, and embedded in paraffin. It was then sectioned into 4-micron thin slices, stained using a Hematoxylin and Eosin Staining Kit (Servicebio), and observed and photographed under a fluorescence microscope (Olympus). In the immunohistochemistry experiment, the sections were dewaxed and then immersed in 3% H_2O_2 at room temperature for 30 min. The sections were washed with PBS and blocked with serum at room temperature for 30 min, followed by overnight incubation with the primary antibody at 4 °C. Subsequently, the sections were incubated with the secondary antibody at room temperature for 30 min. Finally, the sections were observed and photographed using a fluorescence microscope (Olympus).

Statistical analysis

Each data was obtained independently three times. The data for each group are presented as mean ± standard deviation. A one or two way ANOVA were applied to assess differences between groups. The *P* value less than 0.05 is considered statistically significant. Visualization and significance analysis were carried out using Graph Pad Prism.

Results

Targets prediction

The 2D structure of DET is displayed in Fig. 2A. SwissTargetPrediction identified a total of 98 potential targets for DET, while 5710 targets associated with NSCLC were obtained from the GeneCards database. Intersection analysis revealed 52 overlapping targets between DET and NSCLC, as illustrated in the Venn diagram in Fig. 2B. Using the STRING database, the PPI network for the 52 intersecting targets was constructed, with the results illustrated in Fig. 2C. The top 10 target genes are shown in Fig. 2D.

Enrichment analysis

Enrichment analysis was performed using the DAVID database with the 52 overlapping targets of DET and NSCLC. The results revealed that these potential targets of DET in relation to NSCLC were enriched in 164 biological processes (BP), primarily involving inflammatory response and protein phosphorylation; 40 cellular components (CC), mainly including the cytoplasm and plasma membrane; and 44 molecular functions (MF), predominantly involving enzyme binding and protein kinase activity (Fig. 3A). Additionally, KEGG enrichment analysis identified 97 pathways associated with the anti-NSCLC effects of DET. The functional enrichment results

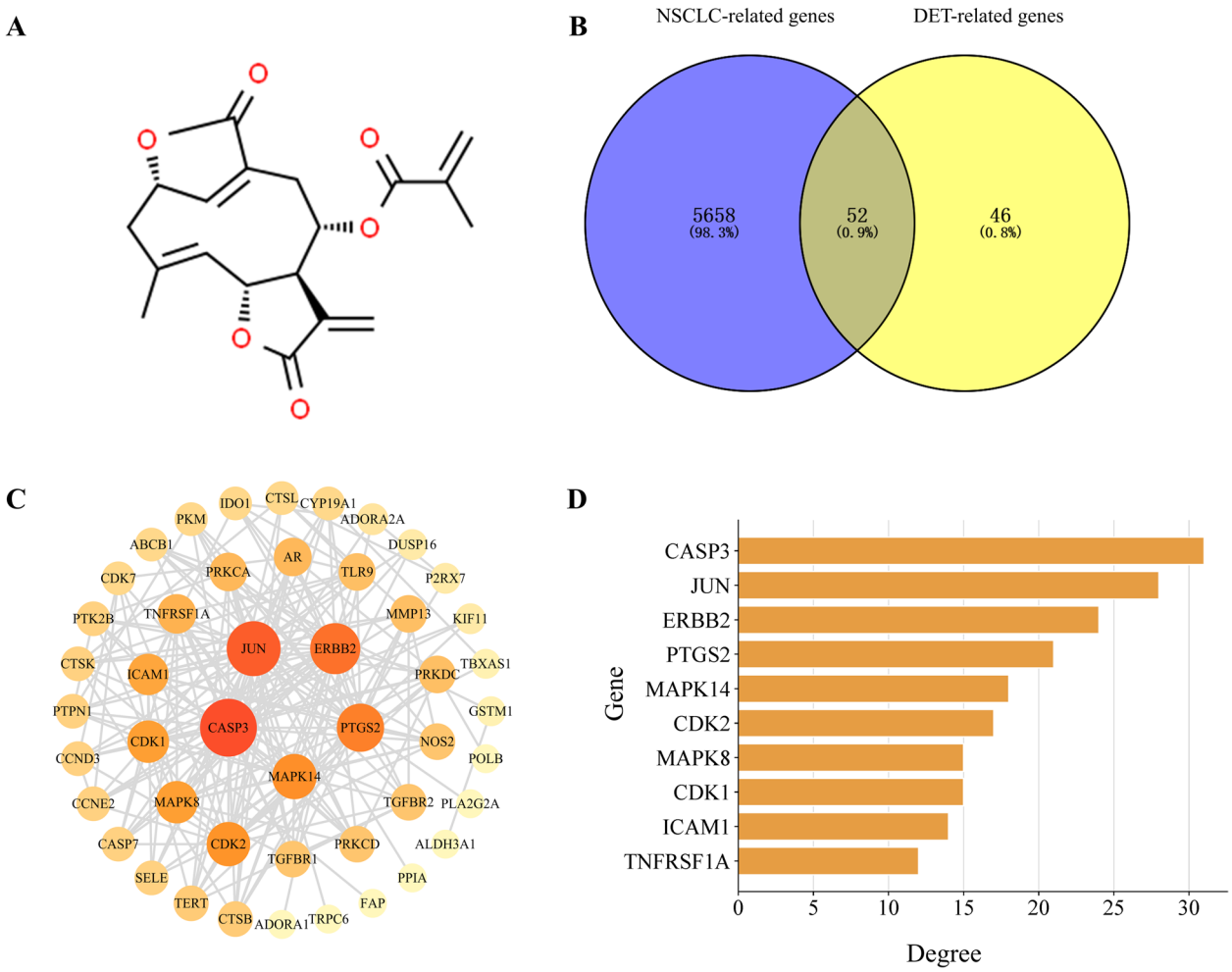

Fig. 2 The prediction of targets for DET against NSCLC. **A** The 2D chemical structure of DET. **B** Venn diagram of potential targets of DET against NSCLC. **C** The PPI network is constructed by Cytoscape. The node size and color stand for the size of the degree. Node size and color are proportional to its degree. **D** The bar chart of the top ten target genes arranged by degree

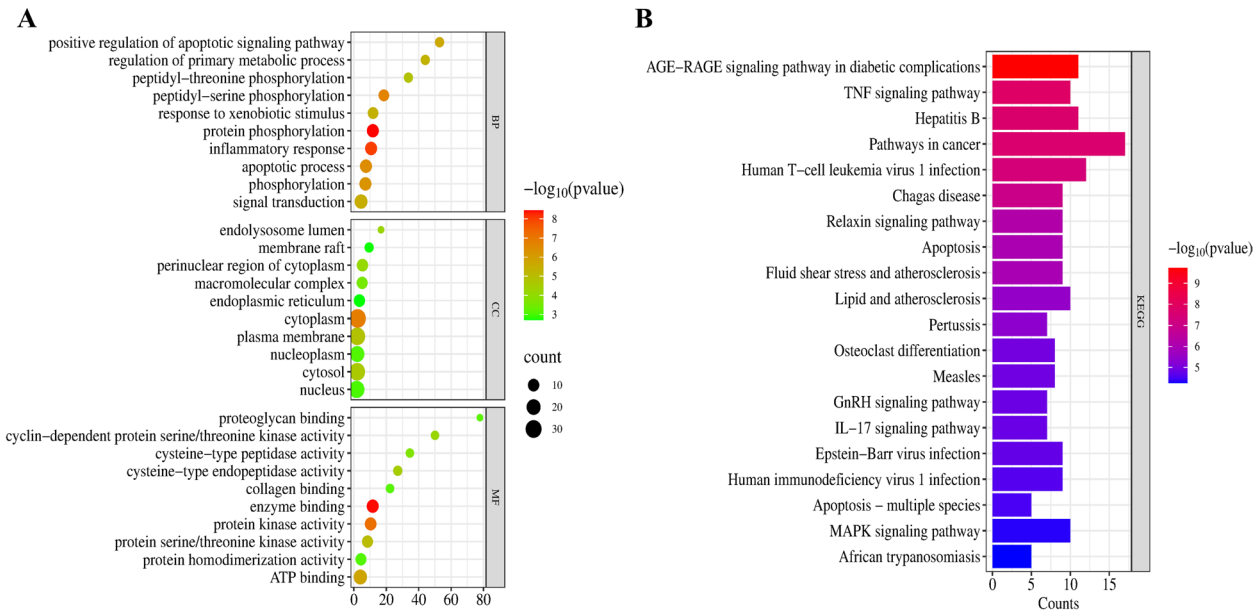

Fig. 3 Enrichment analysis of target genes of DET against NSCLC. **A** GO enrichment bubble diagram. Node color is displayed in a gradient from red to green in descending order of the *P* value. The size of the nodes is arranged in ascending order of the number of genes. **B** KEGG enrichment bar chart. The color of the bars is displayed in a gradient from red to blue, arranged in descending order of the *P* value

indicated that the primary pathways were the AGE-RAGE signaling pathway and the TNF signaling pathway (Fig. 3B), suggesting their critical roles in mediating the anti-NSCLC effects of DET. Notably, the significantly enriched genes from the AGE-RAGE and TNF pathways included CASP3, Bax, Bcl2, TNFα, JUN, ICAM1, and PTGS2. This finding suggests that DET exerts its anti-NSCLC effects through modulation of multiple targets and pathways (Fig. 4).

Molecular docking

Following the PPI network results (Fig. 2B), we selected the top five targets for molecular docking: CASP3, JUN, ERBB2, PTGS2, and MAPK14. A binding energy below −5 kcal/mol suggests strong binding activity; the greater the absolute value of the binding energy, the more effectively DET binds to the targets [28, 29]. The binding energies between DET and the hub targets are presented in Table 2. Visualization of five target-DET pairs with binding energies below −5 kcal/mol revealed that CASP3, JUN, ERBB2, PTGS2, and MAPK14 show significant potential for targeted NSCLC treatment (Fig. 5).

DET inhibits H460 cells proliferation

In the MTT assay, the NSCLC cell line H460 (logarithmic growth phase) and the normal human bronchial epithelial cell line BEAS- 2B were used. The results indicated that DET exhibited a potent inhibitory effect on the proliferation of H460 cells, whereas BEAS- 2B cells exhibited lower sensitivity to DET compared to H460 cells (Fig. 6A). Furthermore, colony formation assays are a crucial method for assessing cellular proliferation capacity. H460 cells were treated with various concentrations of DET for 10 days to assess the size and number of the resulting cell colonies. The results demonstrated that both the number and size of cell colonies decreased with the increasing DET concentration. These findings confirm that DET can significantly inhibit the proliferation of H460 cells (Fig. 6B).

DET inhibits H460 cells migration

H460 cells were treated with different concentrations of DET to evaluate changes in cell migration rates. The results showed that DET significantly reduced the cell migration rate at a concentration of 10 μM compared to the control group ($P < 0.05$). Treatment with higher concentrations of DET (20 and 40 μM) resulted in a further, more pronounced reduction in H460 cell migration ($P < 0.01$). These findings confirm that DET inhibits the lateral migration capability of H460 cells (Fig. 6C).

DET induced apoptosis of H460 cells

The study investigated the induction of apoptosis in H460 cells following a 24-h treatment with DET. To evaluate the effect of DET on apoptosis, TUNEL and DAPI staining techniques were employed. TUNEL staining, a well-established method for detecting apoptotic cells, identifies cells undergoing apoptosis through the

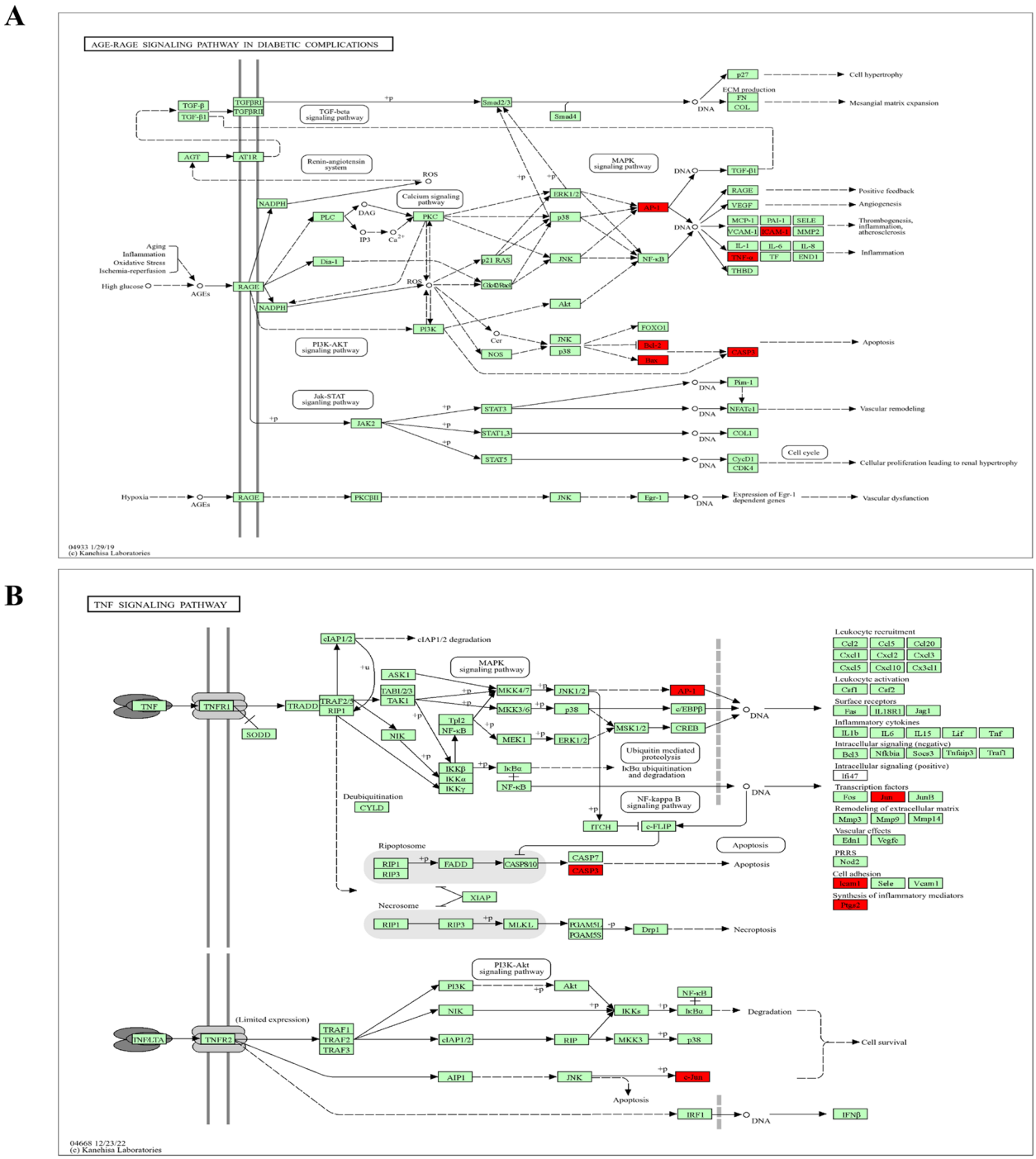

Fig. 4 KEGG enrichment analysis of the 52 potential therapeutic targets. **A** AGE-RAGE signal pathway. **B** TNF signal pathway (red nodes represent overlapping targets in the pathway)

terminal labeling of nucleic acid fragments, typically visualized as green fluorescent puncta. The results from TUNEL staining demonstrated that the apoptosis rates in H460 cells treated with 20 and 40 μM DET were significantly higher compared to the DMSO control group ($P < 0.05$) (Fig. 6D). Furthermore, the analysis revealed a positive correlation between DET concentration and the number of TUNEL positive cells, indicating that the proportion of apoptotic cells increases with increasing DET concentration.

Table 2 Results of molecular docking between DET and hub target proteins

Target	Affinity (kcal/mol)	PDB ID
CASP3	− 6.7	1 NMS
JUN	− 5.5	5 TO1
ERBB2	− 7.6	3PPO
PTGS2	− 7.1	5IKQ
MAPK14	− 7.7	3ZS5

Impact of DET on mRNA and protein levels of associated genes in vitro

The KEGG enrichment analysis results indicate that the AGE-RAGE and TNF signaling pathways are involved in the mechanism by which DET acts against NSCLC. mRNA expression levels of several targets, such as CASP3, Bax, Bcl2, JUN, PTGS2, and ICAM1, were measured using RT-qPCR. DET was found to decrease levels of Bcl2, JUN, TNFα, PTGS2 and ICAM1, and increase CASP3 and Bax levels. The results were shown in Fig. 7A ($P < 0.05$). meanwhile, the protein expression levels of CASP3, Bax, and Bcl2 showed a similar pattern to the mRNA levels ($P < 0.05$) (Fig. 7B).

Given that TNF-α activates adhesion molecules, such as ICAM1, via the NF-κB signaling pathway, and considering the close association between TNF-α secretion/expression and NF-κB activation, we further investigated the expression levels of NF-κB (p65) and its phosphorylated form (p-p65) [30]. Western blot analysis demonstrated that, after 24 h of DET treatment, the ratios of p-p65 to GAPDH and p-p65 to total p65 were significantly decreased in H460 cells (Fig. 7C) ($P < 0.05$). These findings suggest that DET effectively inhibits the phosphorylation of p65 in H460 cells.

DET inhibits tumor growth in vivo

We utilized H460 xenograft mice models to examine the impact of DET on tumor growth in vivo. After tumor implantation, DET was administered to the H460 tumor-bearing mice via gavage. The negative control group received PBS (0.5% CMC-Na), while the positive group was treated with 5-FU. The results indicate that 20 mg/kg DET significantly suppressed the growth of H460 tumors in mice compared to the negative control group ($P < 0.01$) (Fig. 8A). No significant differences were observed among the other treatment groups. Compared to the control group, DET treatment did not significantly affect body weight, whereas 5-FU significantly reduced body weight ($P < 0.05$) (Fig. 8B). These findings suggest that DET exhibits minimal side effects in mice, with no significant differences observed compared to the model group ($P > 0.05$) (Fig. 8B). Following the final measurement, the mice were euthanized by cervical dislocation, and tumor tissues were promptly excised. The results demonstrated that both the DET group and the 5-FU group exhibited a significant reduction in tumor size and weight compared to the control group ($P < 0.05$) (Fig. 8C and D).

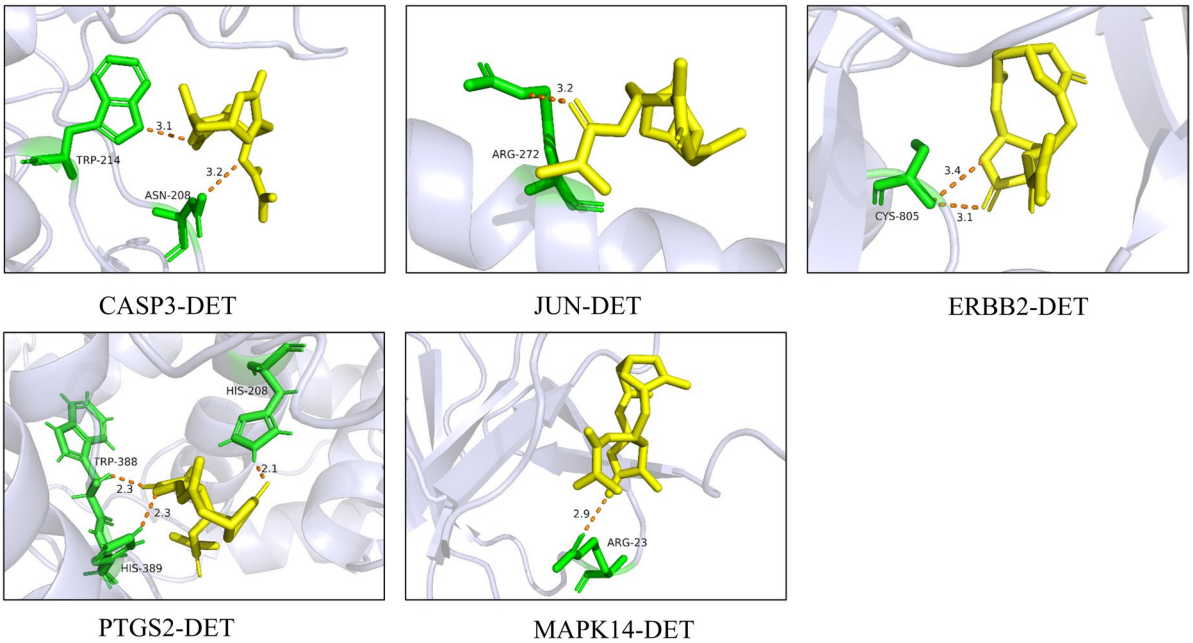

Fig. 5 Molecular docking diagram of DET and hub target proteins

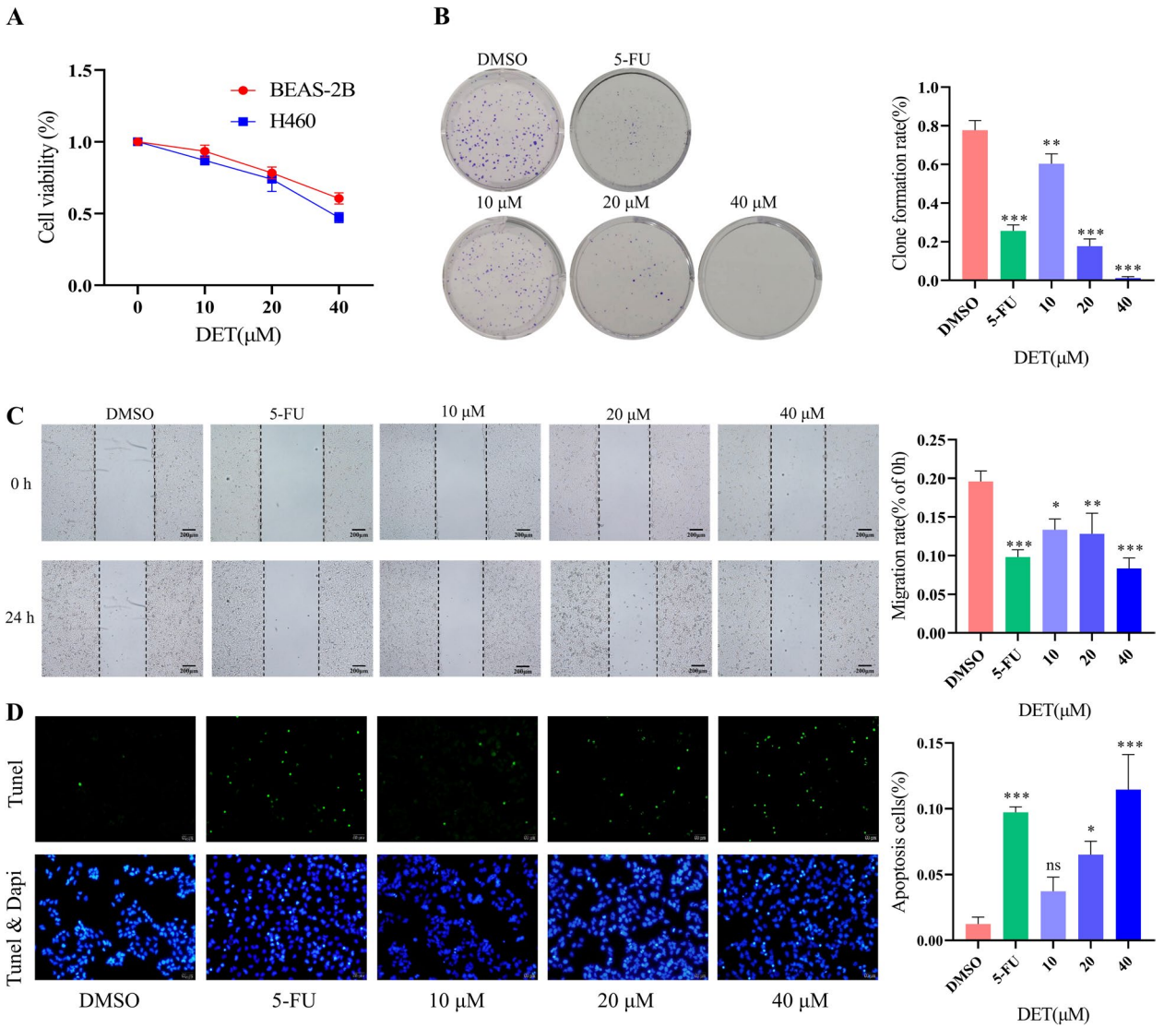

Fig. 6 DET inhibits H460 cells proliferation, migration and induces cell apoptosis in vitro. **A** H460 and BEAS- 2B cells were exposed to a culture medium containing various concentrations of DET for 24 h. The cell viability was measured using the MTT assay. **B** Cell colony-forming growth assay detection of cell colony formation ability. The colonies were counted and captured. **C** The migration of H460 cells was determined using a wound-healing assay. Migrating H460 cells were determined after 24 h of DET treatment. The area filled with H460 cells that entered the middle blank fields was calculated. **D** DET induced apoptosis of H460 cells. The apoptosis-positive cells were stained with Tunel staining kit. All Data are represented as mean ± SD ($n = 3$). *$P < 0.05$, **$P < 0.01$, ***$P < 0.001$, ns = no significant differences versus the non-treated group

In vivo mechanisms of tumor suppression by DET

HE staining revealed nuclear fragmentation following DET and 5-FU treatment. Subsequently, immunohistochemical analysis was performed to assess the levels of cellular proliferation, migration, and apoptosis in tumor tissues by measuring the expression of Ki67, E-cad and CASP3 in tissue sections. The results indicated that the positive rates of E-cad and CASP3 in the 20 mg/kg DET group and the 5-FU treatment group were significantly higher than those in the control group. Conversely, the Ki67 positive rates in these two treatment groups were significantly lower ($P < 0.05$) (Fig. 9).

The expression levels of Bcl2, ICAM1, JUN, PTGS2 and TNFα were decreased ($P < 0.05$). Concurrently, the levels of CASP3 and Bax proteins were increased following treatment with DET (Fig. 10) ($P < 0.05$). These results suggest that DET may inhibit tumor proliferation and promote apoptosis by modulating the targets associated with the AGE-RAGE and TNF signaling pathways.

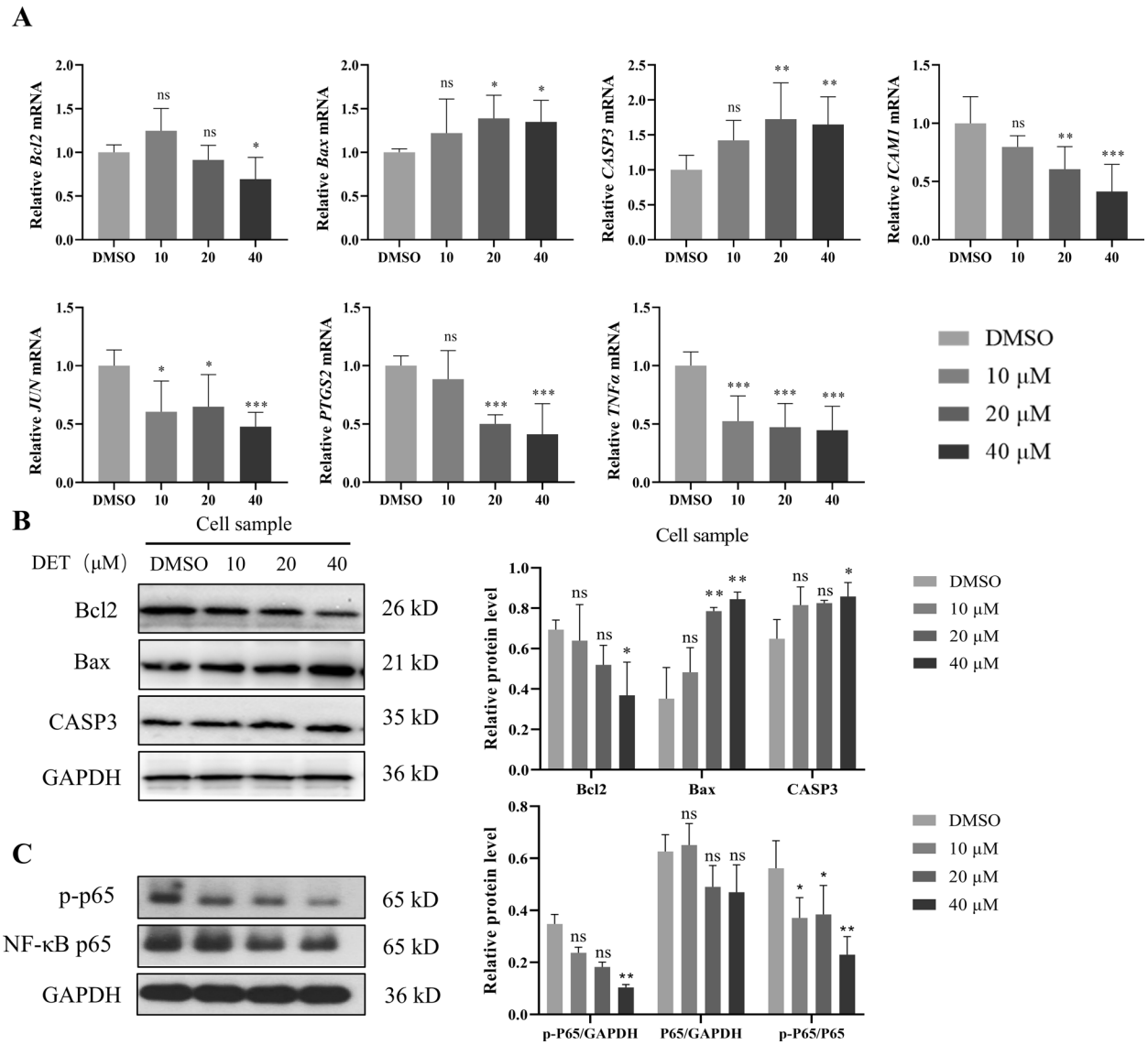

Fig. 7 mRNA and Protein expression in H460 cells after DET intervention in vitro. **A** RT-qPCR analysis of Bcl2, Bax, CASP3, ICAM1, JUN, PTGS2 and TNFα mRNA expression in H460 cells after stimulation with DET (10, 20 and 40 μM) for 24 h. **B** Western blotting analysis of Bcl2, Bax and CASP3 protein expression in H460 cells after stimulation with DET (10, 20 and 40 μM) for 24 h. **C** Western blotting analysis of p-p65 and NFκB(p65) protein expression in H460 cells after stimulation with DET (10, 20 and 40 μM) for 24 h.All Data are represented as mean ± SD (n = 3). *$P < 0.05$, **$P < 0.01$, ***$P < 0.001$, ns = no significant differences versus the non-treated group

Discussion

Traditional Chinese medicine (TCM) possesses notable advantages, including abundant natural resources, intrinsic purity, low toxicity, and high efficacy in disease treatment, which have garnered significant attention in recent years [31]. At present, nearly half of all cancer chemotherapeutic agents come from natural products [32]. Although previous research have explored the antitumor effects of DET in breast cancer [20], colon cancer [16, 33], pancreatic cancer [17], its role in non-small cell lung cancer (NSCLC) remains relatively underexplored. The anticancer mechanism of DET is complex; therefore, and a singular focus on isolated signaling pathways is insufficient to comprehensively elucidate its effects. To address this gap, the present study employed an integrated approach combining network pharmacology with experimental validation to investigate the mechanisms and therapeutic potential of DET in NSCLC.

Network pharmacology provides a systematic framework to bridge the connections between drugs, targets, and diseases, enabling a holistic exploration of the mechanisms underlying traditional Chinese medicine. Molecular docking, a computational technique, further facilitates the identification of promising natural

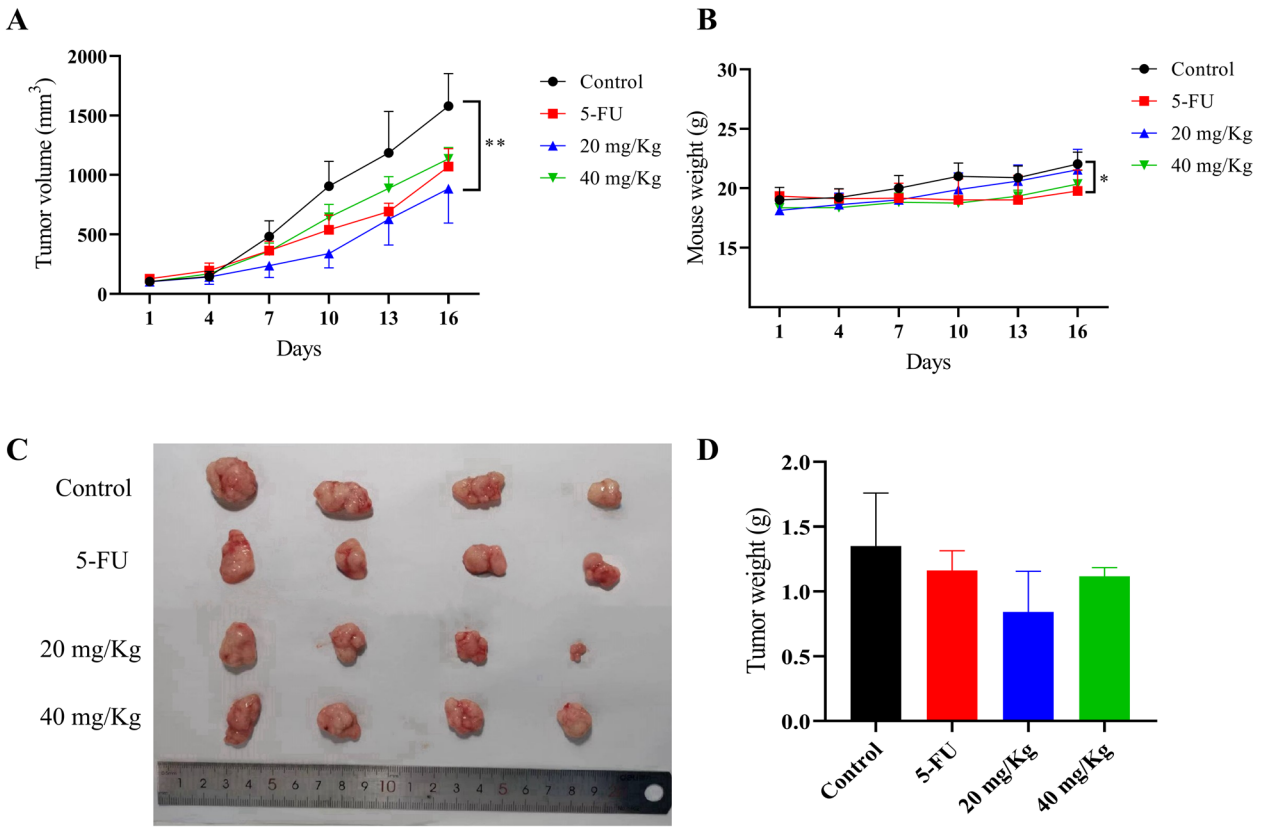

Fig. 8 DET inhibited tumor growth in vivo. **A, C, D** DET inhibited H460 mouse xenograft tumor growth. **B** DET had no effect on mouse weight. Data are represented as mean ± SD (n = 4). *$P < 0.05$, **$P < 0.01$

compounds and predicts molecular interactions between ligands and their targets, thereby accelerating the drug discovery process [23].

In this research, we discovered 52 overlapping genes, and through PPI network analysis, we found 5 hub genes: CASP3, JUN, PTGS2, MAPK14, and ERBB2, which likely connect DET activity to effective NSCLC treatment. Additionally, GO analysis indicated that these candidate target genes are linked to enzyme activity, metabolism, and immune responses. Furthermore, KEGG enrichment analysis revealed that DET is involved in regulating cancer-related signaling pathways, including AGE-RAGE and TNF. Previous studies have demonstrated that the AGE-RAGE and TNF pathways are closely associated with tumor proliferation, growth, and migration [34–36].

Finally, we confirmed the binding capability of the 5 hub genes related to NSCLC and DET using molecular docking. The results demonstrated stable interactions between the ligands and proteins. Specifically, the binding energy values for DET with the target genes CASP3, JUN, PTGS2, MAPK14, and ERBB2 were all less than −5.5 kcal/mol, suggesting strong binding activity and the formation of a stable binding conformation.

The five hub genes were associated with the treatment of NSCLC. CASP3 serves as a primary executor of apoptosis, requiring conversion into its active form, cleaved CASP3, to effectively carry out the apoptotic process [37]. Remarkably, apoptosis induction is not solely contingent upon CASP3 expression levels, but is also intricately linked to the modulation of the Bcl2 family of apoptosis-regulating proteins [38]. Additionally, it has been demonstrated that DET activated both extrinsic and intrinsic apoptosis pathways in NSCLC (A549) cells [18]. Consequently, this investigation did not merely assess the mRNA and protein expression levels of CASP3 in cellular and tissue samples; it also augmented the analysis by including the mRNA and protein expressions of Bcl2 and Bax. The results showed that DET not only promoted apoptosis of H460 cells at the cellular level, but also promoted apoptosis in the mouse model. Our study elucidates that DET considerably augments apoptosis in H460 cells via the regulation of CASP3 and Bcl2 family proteins, delivering substantial experimental evidence and promising therapeutic candidates for the development of new NSCLC treatment paradigms. And also, this

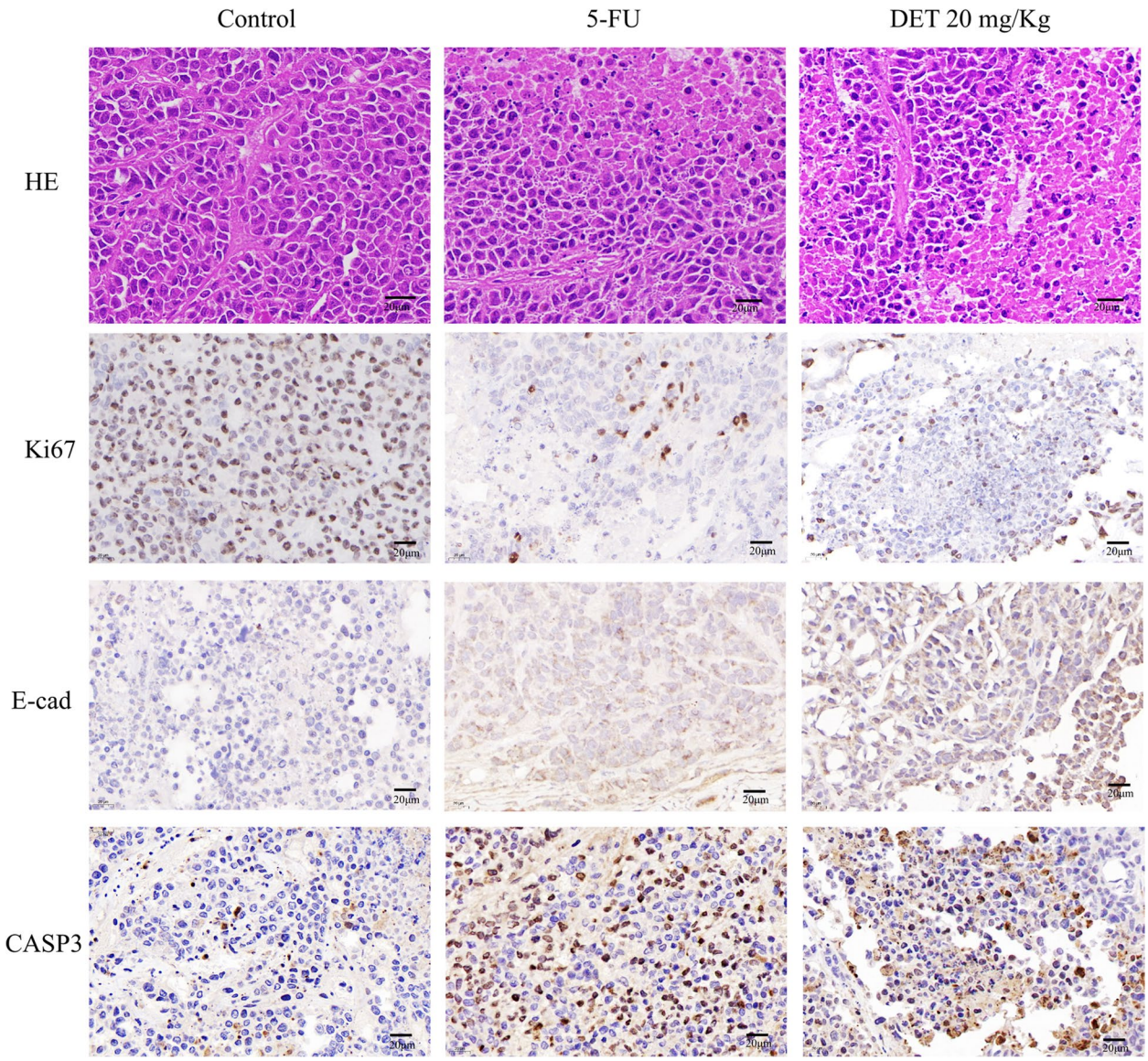

Fig. 9 DET inhibits tumor proliferation, migration and induces apoptosis in vivo. The expressions of Ki67, E-cad and CASP3 in tumor tissues were detected by immunohistochemistry. (400 ×)

research result is consistent with the conclusions of Vivek Pandey et al. [39].

JUN, a transcription factor with a leucine zipper motif, regulates cell proliferation, survival, and differentiation by forming heterodimeric activator protein- 1 (AP- 1) complexes with members of the Fos family [40]. AP- 1, in turn, activates downstream target genes such as cyclin D1, which drives cell cycle progression and promotes cancer cell proliferation [41].

PTGS2, also known as cyclooxygenase- 2 (COX- 2), operates as the pivotal rate-limiting enzyme in the enzymatic pathway that converts arachidonic acid into prostaglandins [42]. COX2 is found to be overexpressed in lung cancer and various other malignant tumors, where it plays a role in regulating tumor angiogenesis and enhancing the growth and migration of cancer cells [43].

It is noteworthy that the AGE-RAGE signaling pathway has an association with the expression of inflammatory factors like TNFα, and that elevated inflammatory factor release contribute to the development of cancer [44]. In tumor microenvironments, inflammatory markers such as TNF-α and ICAM1 are frequently overexpressed, and

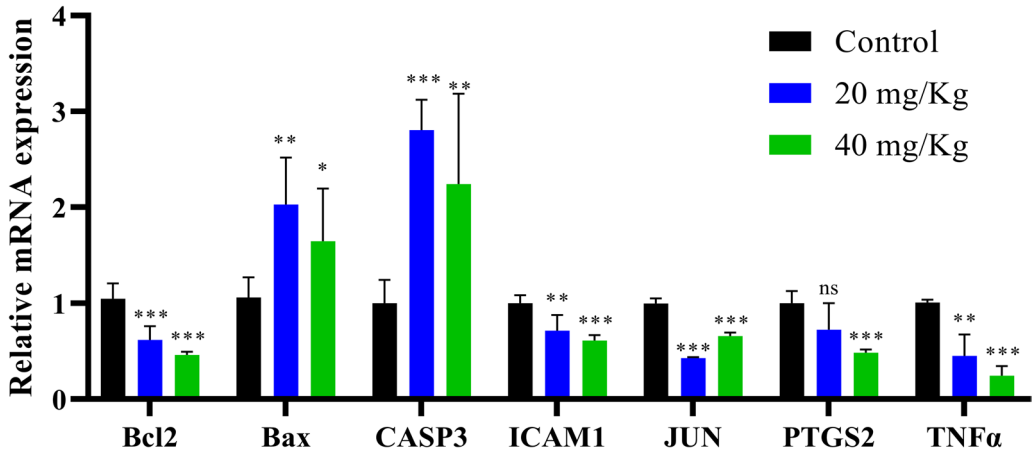

Fig. 10 mRNA expression in vivo after DET treatment. RT-qPCR analysis of Bcl2, Bax, CASP3, ICAM1, JUN, PTGS2 and TNFα mRNA expression in H460 tumor tissue after stimulation with DET (20 and 40 mg/Kg). Data are represented as mean ± SD (n = 3). *$P < 0.05$, **$P < 0.01$, ***$P < 0.001$, ns = no significant differences versus the non-treated group

their dysregulation promotes tumor growth and metastasis [45–47]. To further elucidate the anti-inflammatory effects of DET, we examined the expression levels of ICAM1 and TNF-α following DET treatment. Our data revealed a marked decline in the mRNA expression level of TNF-α within both tumor cells and tissues following DET exposure. This suggests that DET mitigates inflammation within H460 cells and their associated tissues, thereby suppressing cancer cell proliferation and migration (Fig. 11).

Nuclear factor-kappa B (NF-κB) is a transcription factor composed of subunits such as p50, p65, and IκBα, which plays a pivotal role in various physiological processes, including inflammation, cell proliferation, angiogenesis, and tumorigenesis [48]. The activation of NF-κB is primarily mediated by the degradation of IκBα through

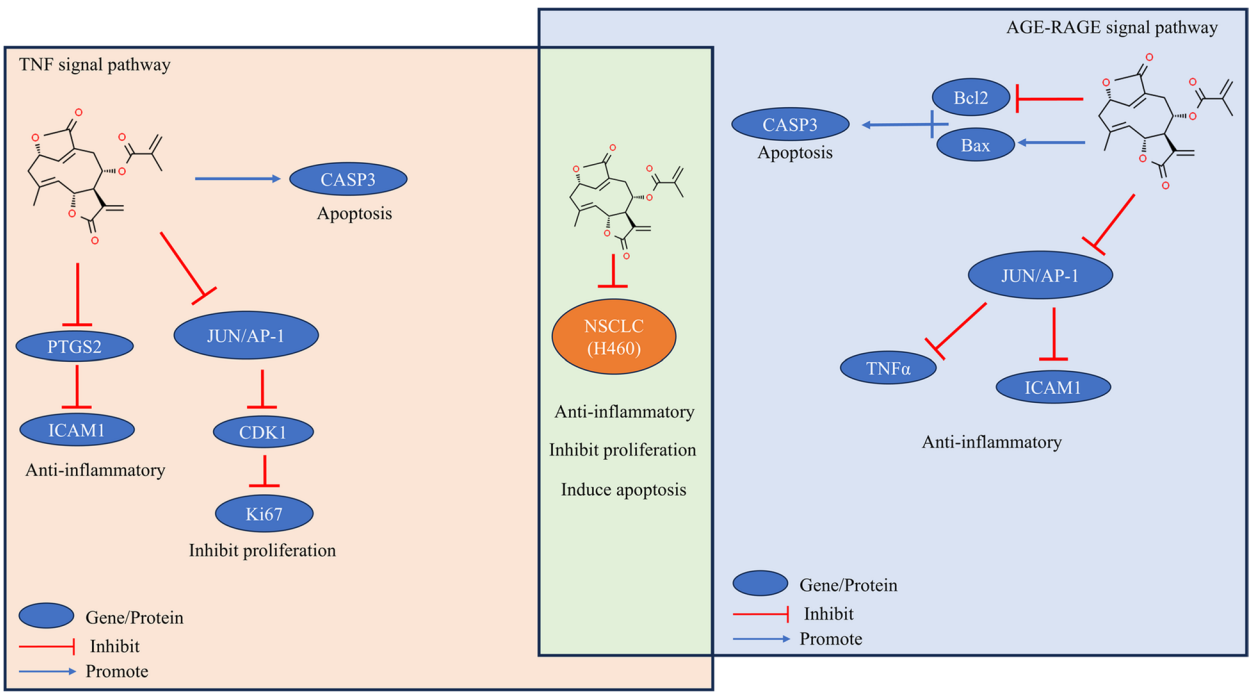

Fig. 11 A schematic diagram of DET inhibits the proliferation, inflammation and induces apoptosis of NSCLC by suppressing TNF and AGE-RAGE signal pathway

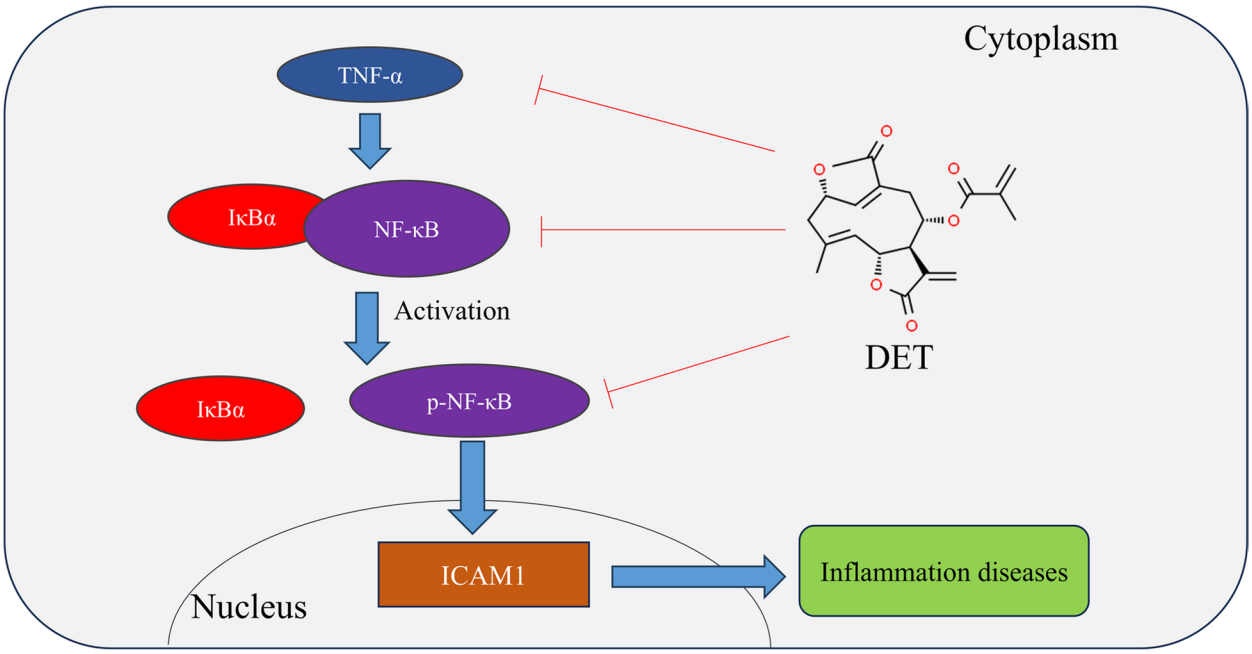

Fig. 12 Schematic illustration of the mechanism by which DET inhibits TNF-α-induced ICAM- 1 expression through suppression of NF-κB activity

the IKK complex, leading to the release of p-p65 and its translocation into the nucleus, where it binds to DNA sequences to regulate the transcription of target genes such as ICAM1 [30, 49] (Fig. 12). NF-κB is constitutively activated in various cancers (e.g., lung cancer, breast cancer, prostate cancer), promoting tumor growth, metastasis, and angiogenesis. Additionally, NF-κB is a major downstream target of the TNF-α signaling pathway, and inhibition of NF-κB activation can induce apoptosis and suppress the progression of inflammation-related diseases, such as arthritis [50, 51]. Research on the NF-κB signaling pathway not only enhances our understanding of the mechanisms underlying tumorigenesis but also provides molecular biomarkers for early intervention and prognostic evaluation in diseases such as cancer [52].

In addition, interestingly, PPI results from network pharmacological analysis showed that DET may also affect the cell cycle process of lung cancer by regulating the expression levels of CDK1, CDK2 and MAPK14. Previous studies have reported that DET can block the cell cycle by regulating the expression of cyclins [14, 53]. However, whether DET can block the cell cycle of NSCLC by regulating the mRNA and protein expression levels of CDK1, CDK2 and MAPK14 remains to be further studied.

In summary, DET can exert antitumor activity on NSCLC cell line (H460) in vitro and in vivo by influencing the expression of CASP3, Bax, Bcl2, PTGS2, JUN, NF-κB, ICAM1 and TNF-α in AGE-RAGE and TNF signaling pathways. These findings provide compelling experimental evidence supporting DET's therapeutic potential in NSCLC treatment.

Conclusion

In this pioneering study, we employed an integrated approach combining network pharmacology analysis with experimental validation to elucidate the molecular mechanisms underlying DET's therapeutic effects against NSCLC. Our in vitro and in vivo experimental results demonstrate that DET can effectively inhibit the growth and migration of NSCLC cells and promote apoptosis. Notably, we identified that DET's therapeutic efficacy is predominantly mediated through the modulation of AGE-RAGE and TNF signaling pathways. These findings not only advance our understanding of DET's mechanism of action but also provide compelling experimental evidence supporting its potential development as a therapeutic agent for NSCLC treatment. This research establishes a robust foundation for future clinical investigations and therapeutic applications of DET in NSCLC management.

Abbreviations

DET	Deoxyelephantopin
NSCLC	Non-small cell lung cancer
SCLC	Small cell lung cancer
GO	Gene Ontology
KEGG	Kyoto Encyclopedia of Genes and Genomes
PPI	Protein-protein interaction
CC	Cellular component
BP	Biological process
MF	Molecule function
DMEM	Dulbecco's Modified Eagle Medium

5-FU	5-Fluorouracil
RT-qPCR	Quantitative reverse-transcription polymerase chain reaction
WB	Western blotting
DAVID	Database for Annotation, Visualization and Integrated Discovery
TNF	Tumor necrosis factor
TNFα	Tumor necrosis factor α
NF-κB	Nuclear factor-kappa B
IκBα	Inhibitor of Kappa B Alpha
IKK	IκB Kinase
CDK	Cyclin Dependent Kinase
MAPK	Mitogen-activated protein kinase
PTGS2	Prostaglandin H synthase 2
COX2	Cyclooxygenase 2
ICAM1	Intercellular adhesion molecule 1

Supplementary Information

The online version contains supplementary material available at https://doi.org/10.1186/s12885-025-14066-3.

Supplementary Material 1.

Supplementary Material 2.

Acknowledgements
Thank you to the School of Biology and Food Engineering at Fuyang Normal University and the Key Laboratory of Environmental Hormones and Reproductive Development of Anhui Province for their support of this research.

Authors' contributions
A:Wu shenjia, B:Guo ying, C:Wang rong. C provided the overall framework and research ideas for the paper and offered revision suggestions for the writing. B participated in some animal and RT-qPCR validation experiments and collected and summarized the experimental data. A was the main executor of the paper writing and experimental validation. †Shenjia Wu and Ying Guo contributed equally to this work.

Funding
This research was supported by the Innovative Research Team in the University of Anhui Province, China. (Project Number: 2022 AH010079).

Data availability
Data is provided within the manuscript or supplementary information files.

Declarations

Ethics approval and consent to participate
The animal experiments involved in this study have been reviewed and approved by the Biomedical Ethics Committee of Fuyang Normal University.

Consent for publication
Not applicable.

Competing Interests
The authors declare no competing interests.

Author details
[1]School of Biology and Food Engineering, Fuyang Normal University, Fuyang Anhui 236041, China. [2]Anhui Province Key Laboratory of Embryo Development and Reproductive Regulation, Fuyang Normal University, 100 Qinghe West Road, Fuyang Anhui 236041, China.

Received: 4 October 2024 Accepted: 1 April 2025
Published online: 21 April 2025

References

1. Sung H, Ferlay J, Siegel RL, Laversanne M, Soerjomataram I, Jemal A, Bray F. Global Cancer Statistics 2020: GLOBOCAN Estimates of Incidence and Mortality Worldwide for 36 Cancers in 185 Countries. CA Cancer J Clin. 2021;71(3):209–49.
2. Schabath MB, Cote ML. Cancer Progress and Priorities: Lung Cancer. Cancer Epidemiol Biomarkers Prev. 2019;28(10):1563–79.
3. Zhou G. Tobacco, air pollution, environmental carcinogenesis, and thoughts on conquering strategies of lung cancer. Cancer Biol Med. 2019;16(4):700–13.
4. Arnold M, Rutherford MJ, Bardot A, Ferlay J, Andersson TM, Myklebust T, Tervonen H, Thursfield V, Ransom D, Shack L, et al. Progress in cancer survival, mortality, and incidence in seven high-income countries 1995–2014 (ICBP SURVMARK-2): a population-based study. Lancet Oncol. 2019;20(11):1493–505.
5. Ma H, Peng F, Xu Y, Bao Y, Hu X, Wang J, Fang M, Kong Y, Dong B, Chen M. Five-year survival rate analysis: the combination of fortnightly-administration of endostar and concurrent chemoradiotherapy versus concurrent chemoradiotherapy in the treatment of inoperable locally advanced non-small cell lung cancer. Ann Palliat Med. 2021;10(7):7560–70.
6. Lei X, Li T, Mao F, Ren F, Tang Q, Cao W, Zu L, Xu S. Lobe-specific analysis of perioperative chemotherapy for non-small cell lung cancer patients. Cancer Med. 2023;12(16):16896–905.
7. Dasari S, Njiki S, Mbemi A, Yedjou CG, Tchounwou PB: Pharmacological Effects of Cisplatin Combination with Natural Products in Cancer Chemotherapy. Int J Mol Sci 2022, 23(3).
8. Zhang Y, Liu L, Zhang M, Li S, Wu J, Sun Q, Ma S, Cai W: The Research Progress of Bioactive Peptides Derived from Traditional Natural Products in China. Molecules 2023, 28(17).
9. Shang L, Wang Y, Li J, Zhou F, Xiao K, Liu Y, Zhang M, Wang S, Yang S. Mechanism of Sijunzi Decoction in the treatment of colorectal cancer based on network pharmacology and experimental validation. J Ethnopharmacol. 2023;302(Pt A): 115876.
10. Jiang Y, Zhang M, Wang L, Zhang L, Ma M, Jing M, Li J, Song R, Zhang Y, Yang Z, et al. Potential mechanisms of osthole against bladder cancer cells based on network pharmacology, molecular docking, and experimental validation. BMC Complement Med Ther. 2023;23(1):122.
11. Gao J, Yang S, Xie G, Pan J, Zhu F. Integrating Network Pharmacology and Experimental Verification to Explore the Pharmacological Mechanisms of Aloin Against Gastric Cancer. Drug Des Devel Ther. 2022;16:1947–61.
12. Hiradeve SM, Rangari VD. A review on pharmacology and toxicology of Elephantopus scaber Linn. Nat Prod Res. 2014;28(11):819–30.
13. Mehmood T, Maryam A, Ghramh HA, Khan M, Ma T: Deoxyelephantopin and Isodeoxyelephantopin as Potential Anticancer Agents with Effects on Multiple Signaling Pathways. Molecules 2017, 22(6).
14. Chan CK, Chan G, Awang K, Abdul Kadir H. Deoxyelephantopin from Elephantopus scaber Inhibits HCT116 Human Colorectal Carcinoma Cell Growth through Apoptosis and Cell Cycle Arrest. Molecules. 2016;21(3):385.
15. Mehmood T, Muanprasat C: Deoxyelephantopin and Its Isomer Isodeoxyelephantopin: Anti-Cancer Natural Products with Multiple Modes of Action. Molecules 2022, 27(7).
16. Ji H, Zhang K, Pan G, Li C, Li C, Hu X, Yang L, Cui H: Deoxyelephantopin Induces Apoptosis and Enhances Chemosensitivity of Colon Cancer via miR-205/Bcl2 Axis. Int J Mol Sci 2022, 23(9).
17. Ji D, Hou L, Xie C, Feng H, Bao D, Teng Y, Liu J, Cui T, Wang X, Xu Y, et al. Deoxyelephantopin Suppresses Pancreatic Cancer Progression *In Vitro* and *In Vivo* by Targeting linc00511/miR-370-5p/p21 Promoter Axis. J Oncol. 2022;2022:3855462.
18. Kabeer FA, Sreedevi GB, Nair MS, Rajalekshmi DS, Gopalakrishnan LP, Kunjuraman S, Prathapan R. Antineoplastic effects of deoxyelephantopin, a sesquiterpene lactone from Elephantopus scaber, on lung adenocarcinoma (A549) cells. J Integr Med. 2013;11(4):269–77.
19. Farha AK, Dhanya SR, Mangalam SN, Remani P. Anti-metastatic effect of deoxyelephantopin from Elephantopus scaber in A549 lung cancer cells *in vitro*. Nat Prod Res. 2015;29(24):2341–5.
20. Beeran AA, Maliyakkal N, Rao CM, Udupa N. The enriched fraction of Elephantopus scaber Triggers apoptosis and inhibits multi-drug resistance transporters in human epithelial cancer cells. Pharmacogn Mag. 2015;11(42):257–68.

21. Jiashuo WU, Fangqing Z, Zhuangzhuang LI, Weiyi J, Yue S. Integration strategy of network pharmacology in Traditional Chinese Medicine: a narrative review. J Tradit Chin Med. 2022;42(3):479–86.
22. Zhang P, Zhang D, Zhou W, Wang L, Wang B, Zhang T, Li S: Network pharmacology: towards the artificial intelligence-based precision traditional Chinese medicine. Brief Bioinform 2023, 25(1).
23. Pinzi L, Rastelli G: Molecular Docking: Shifting Paradigms in Drug Discovery. Int J Mol Sci 2019, 20(18).
24. Hsieh WH, Liao SW, Chan SM, Hou JD, Wu SY, Ho BY, Chen KY, Tai YT, Fang HW, Fang CY, et al. Lidocaine induces epithelial-mesenchymal transition and aggravates cancer behaviors in non-small cell lung cancer A549 cells. Oncol Lett. 2023;26(2):346.
25. Zhang J, Qi C, Li H, Ding C, Wang L, Wu H, Dai W, Wang C: Exploration of the effect and mechanism of Scutellaria barbata D. Don in the treatment of ovarian cancer based on network pharmacology and *in vitro* experimental verification. Medicine (Baltimore) 2023, 102(51):e36656.
26. Choi HI, An GY, Baek M, Yoo E, Chai JC, Lee YS, Jung KH, Chai YG. BET inhibitor suppresses migration of human hepatocellular carcinoma by inhibiting SMARCA4. Sci Rep. 2021;11(1):11799.
27. Li Z, Zhou H, Xia Z, Xia T, Du G, Franziska SD, Li X, Zhai X, Jin B. HMGA1 augments palbociclib efficacy via PI3K/mTOR signaling in intrahepatic cholangiocarcinoma. Biomark Res. 2023;11(1):33.
28. Xu C, Sun L, Wang H, Sun J, Feng Y, Wang X, Song Z. Identifying the mechanism of polysaccharopeptide against breast cancer based on network pharmacology and experimental verification. BMC Cancer. 2024;24(1):726.
29. Song S, Wen F, Gu S, Gu P, Huang W, Ruan S, Chen X, Zhou J, Li Y, Liu J, et al. Network Pharmacology Study and Experimental Validation of Yiqi Huayu Decoction Inducing Ferroptosis in Gastric Cancer. Front Oncol. 2022;12: 820059.
30. Gao JJ, Hu YW, Wang YC, Sha YH, Ma X, Li SF, Zhao JY, Lu JB, Huang C, Zhao JJ, et al. ApoM Suppresses TNF-α-Induced Expression of ICAM-1 and VCAM-1 Through Inhibiting the Activity of NF-κB. DNA Cell Biol. 2015;34(8):550–6.
31. Hiebl V, Ladurner A, Latkolik S, Dirsch VM. Natural products as modulators of the nuclear receptors and metabolic sensors LXR. FXR and RXR Biotechnol Adv. 2018;36(6):1657–98.
32. Newman DJ, Cragg GM. Natural Products as Sources of New Drugs from 1981 to 2014. J Nat Prod. 2016;79(3):629–61.
33. Chan CK, Supriady H, Goh BH, Kadir HA. Elephantopus scaber induces apoptosis through ROS-dependent mitochondrial signaling pathway in HCT116 human colorectal carcinoma cells. J Ethnopharmacol. 2015;168:291–304.
34. Shi G, Hu Y: TNFR1 and TNFR2, Which Link NF-κB Activation, Drive Lung Cancer Progression, Cell Dedifferentiation, and Metastasis. Cancers (Basel) 2023, 15(17).
35. Wajant H, Siegmund D. TNFR1 and TNFR2 in the Control of the Life and Death Balance of Macrophages. Front Cell Dev Biol. 2019;7:91.
36. Somensi N, Brum PO, de Miranda RV, Gasparotto J, Zanotto-Filho A, Rostirolla DC, da Silva MM, Moreira JCF, Pens Gelain D. Extracellular HSP70 Activates ERK1/2, NF-kB and Pro-Inflammatory Gene Transcription Through Binding with RAGE in A549 Human Lung Cancer Cells. Cell Physiol Biochem. 2017;42(6):2507–22.
37. Lin B, Zhu M, Wang W, Li W, Dong X, Chen Y, Lu Y, Guo J, Li M. Structural basis for alpha fetoprotein-mediated inhibition of caspase-3 activity in hepatocellular carcinoma cells. Int J Cancer. 2017;141(7):1413–21.
38. Chen HC, Kanai M, Inoue-Yamauchi A, Tu HC, Huang Y, Ren D, Kim H, Takeda S, Reyna DE, Chan PM, et al. An interconnected hierarchical model of cell death regulation by the BCL-2 family. Nat Cell Biol. 2015;17(10):1270–81.
39. Pandey V, Tripathi A, Rani A, Dubey PK: Deoxyelephantopin, a novel naturally occurring phytochemical impairs growth, induces G2/M arrest, ROS-mediated apoptosis and modulates lncRNA expression against uterine leiomyoma. Biomedicine & pharmacotherapy = Biomedecine & pharmacotherapie 2020, 131:110751.
40. Ibrahim SAE, Abudu A, Johnson E, Aftab N, Conrad S, Fluck M. The role of AP-1 in self-sufficient proliferation and migration of cancer cells and its potential impact on an autocrine/paracrine loop. Oncotarget. 2018;9(76):34259–78.
41. Ming J, Jiang G, Zhang Q, Qiu X, Wang E. Interleukin-7 up-regulates cyclin D1 via activator protein-1 to promote proliferation of cell in lung cancer. Cancer Immunol Immunother. 2012;61(1):79–88.
42. Patrono C. Cardiovascular effects of cyclooxygenase-2 inhibitors: a mechanistic and clinical perspective. Br J Clin Pharmacol. 2016;82(4):957–64.
43. Simonsson M, Björner S, Markkula A, Nodin B, Jirström K, Rose C, Borgquist S, Ingvar C, Jernström H. The prognostic impact of COX-2 expression in breast cancer depends on oral contraceptive history, preoperative NSAID use, and tumor size. Int J Cancer. 2017;140(1):163–75.
44. Ahmad S, Khan MY, Rafi Z, Khan H, Siddiqui Z, Rehman S, Shahab U, Khan MS, Saeed M, Alouffi S, et al. Oxidation, glycation and glycoxidation-The vicious cycle and lung cancer. Semin Cancer Biol. 2018;49:29–36.
45. Wu Y, Yang Y, Wang L, Chen Y, Han X, Sun L, Chen H, Chen Q. Effect of Bifidobacterium on osteoclasts: TNF-α/NF-κB inflammatory signal pathway-mediated mechanism. Front Endocrinol (Lausanne). 2023;14:1109296.
46. Jiang Y, Zhou J, Zhao J, Hou D, Zhang H, Li L, Zou D, Hu J, Zhang Y, Jing Z. MiR-18a-downregulated RORA inhibits the proliferation and tumorigenesis of glioma using the TNF-α-mediated NF-κB signaling pathway. EBioMedicine. 2020;52: 102651.
47. Huang C, Li N, Li Z, Chang A, Chen Y, Zhao T, Li Y, Wang X, Zhang W, Wang Z, et al. Tumour-derived Interleukin 35 promotes pancreatic ductal adenocarcinoma cell extravasation and metastasis by inducing ICAM1 expression. Nat Commun. 2017;8:14035.
48. Shi Y, Wang SY, Yao M, Sai WL, Wu W, Yang JL, Cai Y, Zheng WJ, Yao DF. Chemosensitization of HepG2 cells by suppression of NF-κB/p65 gene transcription with specific-siRNA. World J Gastroenterol. 2015;21(45):12814–21.
49. Chen L, Lin X, Lei Y, Xu X, Zhou Q, Chen Y, Liu H, Jiang J, Yang Y, Zheng F, et al. Aerobic glycolysis enhances HBx-initiated hepatocellular carcinogenesis via NF-κBp65/HK2 signalling. Journal of experimental & clinical cancer research : CR. 2022;41(1):329.
50. Bakshi HA, Quinn GA, Nasef MM, Mishra V, Aljabali AAA, El-Tanani M, Serrano-Aroca Á, Webba Da Silva M, McCarron PA, Tambuwala MM: Crocin Inhibits Angiogenesis and Metastasis in Colon Cancer via TNF-α/NF-kB/VEGF Pathways. Cells 2022, 11(9).
51. Rundall BK, Denlinger CE, Jones DR. Combined histone deacetylase and NF-kappaB inhibition sensitizes non-small cell lung cancer to cell death. Surgery. 2004;136(2):416–25.
52. Van Waes C. Nuclear factor-kappaB in development, prevention, and therapy of cancer. Clinical cancer research : an official journal of the American Association for Cancer Research. 2007;13(4):1076–82.
53. Chao WW, Cheng YW, Chen YR, Lee SH, Chiou CY, Shyur LF. Phyto-sesquiterpene lactone deoxyelephantopin and cisplatin synergistically suppress lung metastasis of B16 melanoma in mice with reduced nephrotoxicity. Phytomedicine. 2019;56:194–206.

Publisher's Note